JOURNAL OF CATALYSIS 153, 86–93 (1995)

Low-Loaded Palladium on α-Alumina Catalysts: Characterization by Chemisorption, Electron Microscopy, and Photoelectron Spectroscopy

J. Goetz,* M. A. Volpe,† A. M. Sica,† C. E. Gigola,† and R. Touroude*,[1]

*Laboratoire d'Etudes de la Réactivité Catalytique, des Surfaces et Interfaces, URA 1498 du CNRS, Université Louis Pasteur, 4 rue B. Pascal, F-67070 Strasbourg Cedex, France; and †Planta Piloto de Ingeneria Quimica (UNS—CONICET) 12 de Octobre 1842, 8000 Bahia Blanca, Argentina

Received June 9, 1993; revised November 29, 1994

Combined X-ray photoelectron spectroscopy, transmission electron microscopy (TEM), and chemisorption measurements of 0.09–0.30 wt% Pd/α-Al_2O_3 catalysts were performed. $Pd(C_5H_7O_2)_2$ benzene solutions of varying concentrations were used as precursors. It was found that the core level binding energies of Pd were totally independent of the particle size in the 1.5–7.5 nm range, yet correlated with the metal loading. For the samples with Pd concentrations decreasing from 0.30 to 0.09%, a binding energy (BE) shift of about 1 eV toward higher BE has been observed. On the 0.09% Pd sample, a large interaction between metal and support is assumed, leading to the epitaxial growth of the particle. In the 0.30% Pd sample, 6-nm sized bulk-like Pd particles having only a little interaction with the support are obtained. Both types of particles, interactive or noninteractive with the support, are formed in the sample with an intermediate concentration (0.20% Pd) showing a clear bimodal distribution by TEM analysis. A coherent explanation of the results emerges considering that two different phases are obtained when $Pd(C_5H_7O_2)_2$ is deposited on α-alumina; the proportions of these two phases depends upon the concentration of the precursor solution.

INTRODUCTION

The manufacture of polymer grade ethylene requires the elimination of small amounts of acetylenic and diolefinic compounds via selective hydrogenation processes. Pd is the most active and selective metal for these reactions. The competitive adsorption of alkynes or alkadienes and olefines determines the Pd selectivity. The preferred catalysts have a very low metal content in order to avoid high activities and enhance the selectivity while maintaining isothermal reactor conditions. The support is a low surface area alumina designed to suppress polymerization reactions.

Despite the fact that these catalysts are widely used, the relation between the chemical state of the Pd particles and the activity and selectivity for hydrogenation reactions is still unclear. The nature of the support and the method of preparation certainly affect the morphology and the particle size distribution which, in turn, may play a role in the catalytic properties.

Numerous investigations have already been reported on the electronic structure of supported Pd particles using mainly X-ray photoelectron spectroscopy (XPS) measurements (1–4). Most studies deal with model systems prepared by vacuum evaporation of Pd on different substrates. However, there is no agreement regarding the origin of the observed binding energy (BE) shifts. XPS data alone do not provide an unambiguous answer because the shifts may be due to instrinsic electronic properties of the metal or to support effects (5, 6). In this paper we report combined XPS, transmission electron microscopy (TEM), and chemisorption measurements of Pd/α-Al_2O_3 catalysts of varying particle size, in which the metal loading is similar to that found on industrial hydrogenation catalysts. In addition the selected method of preparation leads to a well-dispersed Pd phase favoring a close interaction with the alumina support.

EXPERIMENTAL

Catalyst Preparation

The catalysts were prepared by wet impregnation of α-Al_2O_3 (Rhône–Poulenc, 10 m^2/g, precalcined at 773 K) with benzene solutions of bis-acetylacetonato-palladium ($Pd(C_5H_7O_2)_2$), in accordance with a procedure described by Boitiaux *et al.* (7). Benzene solutions containing 0.7×10^{-3}, 1.45×10^{-3}, and 3.33×10^{-3} g Pd/ml were used to obtain samples with Pd loadings of 0.09, 0.20, and 0.30 wt%, respectively, keeping the solution to support ratio constant. The resulting mixtures were maintained at

[1] To whom correspondence should be addressed.

0021-9517/95 $6.00

room temperature in closed flasks for 72 h with occasional stirring. The samples were then filtered, dried overnight at 383 K, and calcined in air at 573 K for 2 h. Finally they were reduced in flowing hydrogen at the same temperature and for the same period of time. Subsequently, a certain amount of each catalyst was reduced at 773 K for 1 h in order to increase the Pd particle size by metal sintering. The 0.09% Pd sample was reduced at 573 K, already characterized by TEM and H_2 chemisorption, was provided by Aduriz *et al.* (8). Metal loadings were determined by atomic absorption spectroscopy (AAS).

Transmission Electron Microscopy

The particle size distribution was determined by TEM using a Jeol 100 CX instrument operated at 100 kV (Centro Regional de Investigaciones Basicas y Aplicadas de Bahía Blanca, Argentina). Over 100 particles were examined on the TEM micrographs. The average particle size has been calculated as $d = \Sigma\, n_i d_i^3 / \Sigma\, n_i d_i^2$.

When analyses were repeated on a Philips EM 300G instrument operated at 100 kV (Laboratoire de Cristallographie de l'Université Louis Pasteur, Strasbourg, France), the results were in total accordance. The micrograph, reproduced as Fig. 1, was obtained using this last apparatus and the extractive replica technique.

Sorption Measurements

The fraction of exposed Pd atoms was derived from hydrogen sorption measurements performed in a static volumetric apparatus, following the double isotherm method proposed by Benson *et al.* (9). Prior to sorption measurements, the samples were treated in a stream of hydrogen at 573 K for 1 h and evacuated at the same temperature overnight. The first isotherm, measured at room temperature in the 0–14 kPa pressure range, gave the total H_2 uptake.

Subsequently, the catalysts were evacuated for 30 min at the same temperature and a second isotherm was obtained to determine the amount of absorbed and weakly

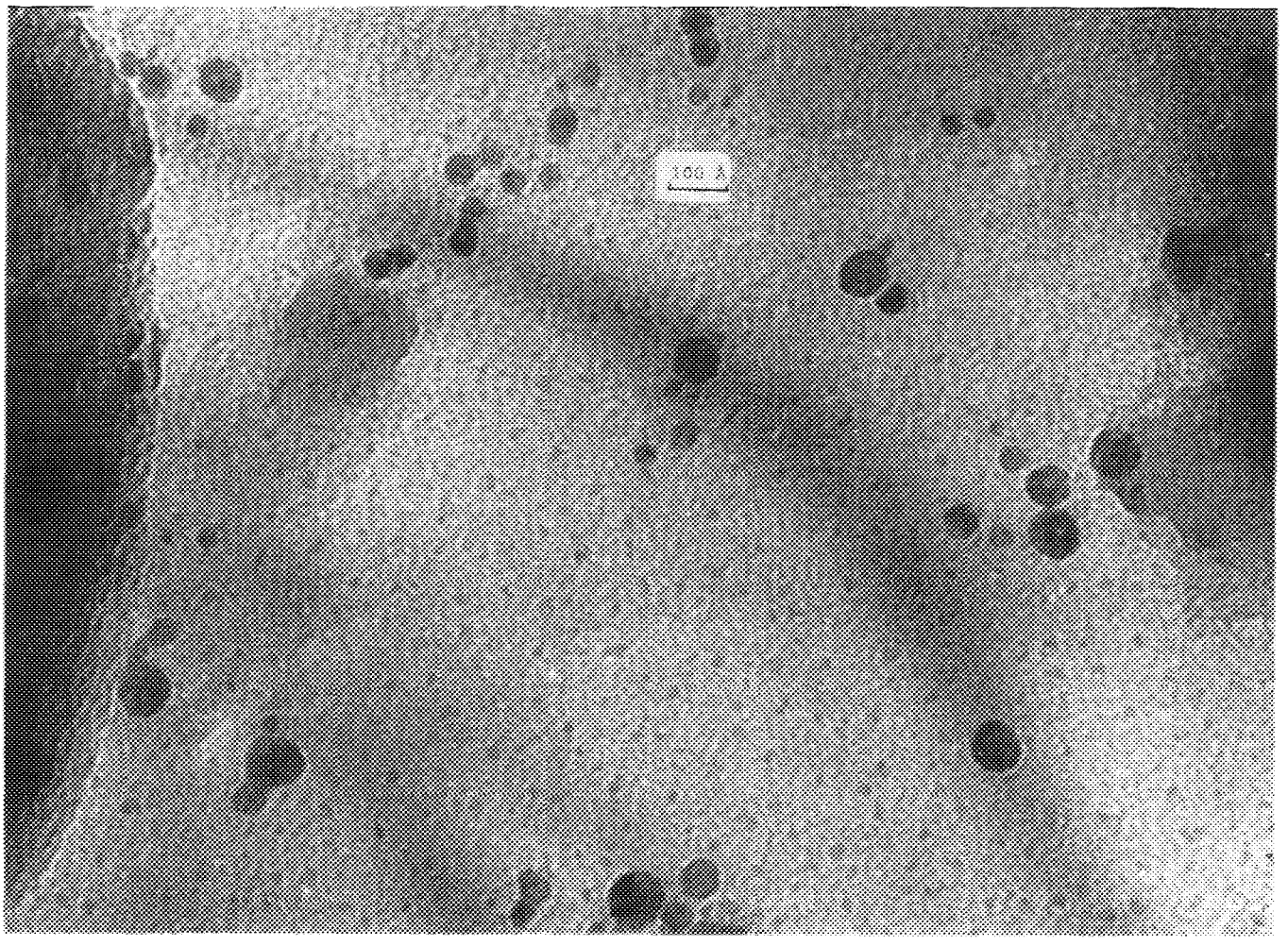

FIG. 1. TEM of Pd/α-Al_2O_3 0.20 wt% sample, reduced at 573 K (Magnification: 10^6).

adsorbed gas removed during the evacuation step. The extent of irreversibly adsorbed gas was obtained by subtracting this contribution from the total uptake. The linear portion of both isotherms was extrapolated to zero pressure to estimate the corresponding uptake values. Assuming that the surface stoichiometry of the irreversibly adsorbed hydrogen is unity, the fraction of exposed Pd atoms is given by $(H/Pd)_{irr}$.

X-ray Photoelectron Spectroscopy

The measurements were performed using a VG Esca III spectrometer with Al$K\alpha$ radiation (1486.6 eV) as incident beam without a monochromator. Before conducting the XPS analysis, the samples already reduced at 573 K, were treated *in situ* at 573 or 773 K for 1 h under 1 atm of hydrogen (1 atm = 1.013×10^5 Pa). After reduction the samples were cooled in hydrogen to room temperature. The pretreatment chamber was then evacuated to 10^{-8} Torr and the sample was transferred to the main chamber, where the vacuum was better than 10^{-9} Torr. In this manner, possible air contamination, which is known to influence the XPS Pd lines in supported Pd catalysts (10), is avoided.

Due to charging effects on the α-Al_2O_3 samples, the XPS peaks were found to shift toward higher BE. Consequently, the Al 2*s* BE was used as a reference to correct the XPS peak positions in all samples. It was fixed at 119.6 eV since Légaré and Frisch (11) found this value referenced to the Fermi level of Pd obtained by metal vapor deposition on a single α-Al_2O_3 crystal. On this sample the Pd BE was found to be 335.2 eV.

It will be noted that using Al 2*s* at 119.6 eV to calibrate the binding energies, the C 1*s* BE was found at 285.6 eV whatever the sample, i.e., the charging corrections using support signals or contaminating carbon lead to the same BE of Pd.

The charging effects were very stable while subjected to X rays, provided the samples were pretreated *in situ* under hydrogen at high temperature. This beneficial effect of the *in situ* pretreatment has already been observed by Noack *et al.* (10). The XPS spectra obtained from several pellets of the same catalyst reveal totally reproducible measurements. We have verified that the binding energies are independent of the X-ray beam intensities when using 5, 10, 20, and 40 mA. All these results indicate that no differential charge effects are occurring.

Spectra were obtained for the O 1*s*, C 1*s*, Al 2*s*, Pd 3*d*, Ca 2*p*, and Pd MVV Auger regions. When the elements were present at very low concentration, as was the case for Pd, 20 scans were accumulated in order to increase the signal to noise ratio. Therefore, the Pd signal was neat, even for the lowest content of metal (Fig. 2). The Al 2*s* line was also scanned in the same manner to extract the experimental Gaussian factor (G) from the lineshape analysis as described below; these so-determined G values are used in the Pd line-fitting procedure.

The lineshape analysis was performed using a homemade curve-fitting program. The fit was made considering Shirley's background substraction (12) and the Doniach-Sunjic Lorentzian asymmetric function (13) which was convoluted with an experimental Gaussian curve (G) that takes into account X-ray source broadening (Al$K\alpha_1$, α_2, α_3, α_4), instrumental resolution, phonon excitation, charging effects and other possible sources of inhomogeneous broadening. For each transition, the binding energies, γ, and α, were measured. An analysis of γ and α is not provided in this paper.

Estimations of the normalized atomic ratios, Pd/Al_{XPS}, were made by relating Pd 3*d* and Al 2*s* peak areas after Shirley's background subtraction, corrected by differences in escape depths λ (a square root approximation was used), in cross section σ (using Scofield's data (14), and in atomic density, ρ. This so-used theoretical correction factor ratio, $(\rho \cdot \sigma \cdot \lambda)_{Al}/(\rho \cdot \sigma \cdot \lambda)_{Pd}$, for the considered XPS lines was found to be in total accord with the experimental one obtained with the same apparatus on a single α-Al_2O_3 crystal from which a thick monolayer of Pd metal had been evaporated (15).

Due to the presence of Ca as an impurity in the alumina support, it was necessary to take into account Ca 2*p* lines and their satellites (due to Al$K\alpha_2$, α_3 X-ray excitation source) which overlap the Pd 3*d*; afterward the deconvolution procedure was applied in order to eliminate the influence of Ca on the area and lineshape. The curve-fitted Pd 3*d* region for the Pd/α-Al_2O_3 samples containing 0.09, 0.20, 0.30% Pd, reduced at 573 K, are shown in Fig. 2.

The use of this deconvolution procedure and the reproducibility of our experiments permit us to estimate the error in BE measurements at ± 0.1 eV whatever the catalyst.

MVV Auger lines were recorded in the 1130–1160 eV range (326.6–335.6 KE range). To extract the rather broad MVV Auger Pd lines in this region we have subtracted a linear background.

A decontaminated Pd foil sample was also used to obtain the reference values for BE (335.2 eV), α (0.09), and γ (0.3). In this case, BE was referenced to the Fermi level and 0.75 eV was obtained as the experimental Gaussian value.

RESULTS AND DISCUSSION

Table 1 summarizes the chemisorption and TEM results for samples reduced at 573 and 773K. The data in Table 1 indicate that a twofold increase in $Pd(C_5H_7O_2)_2$ concentration increases the metal content from 0.1 to

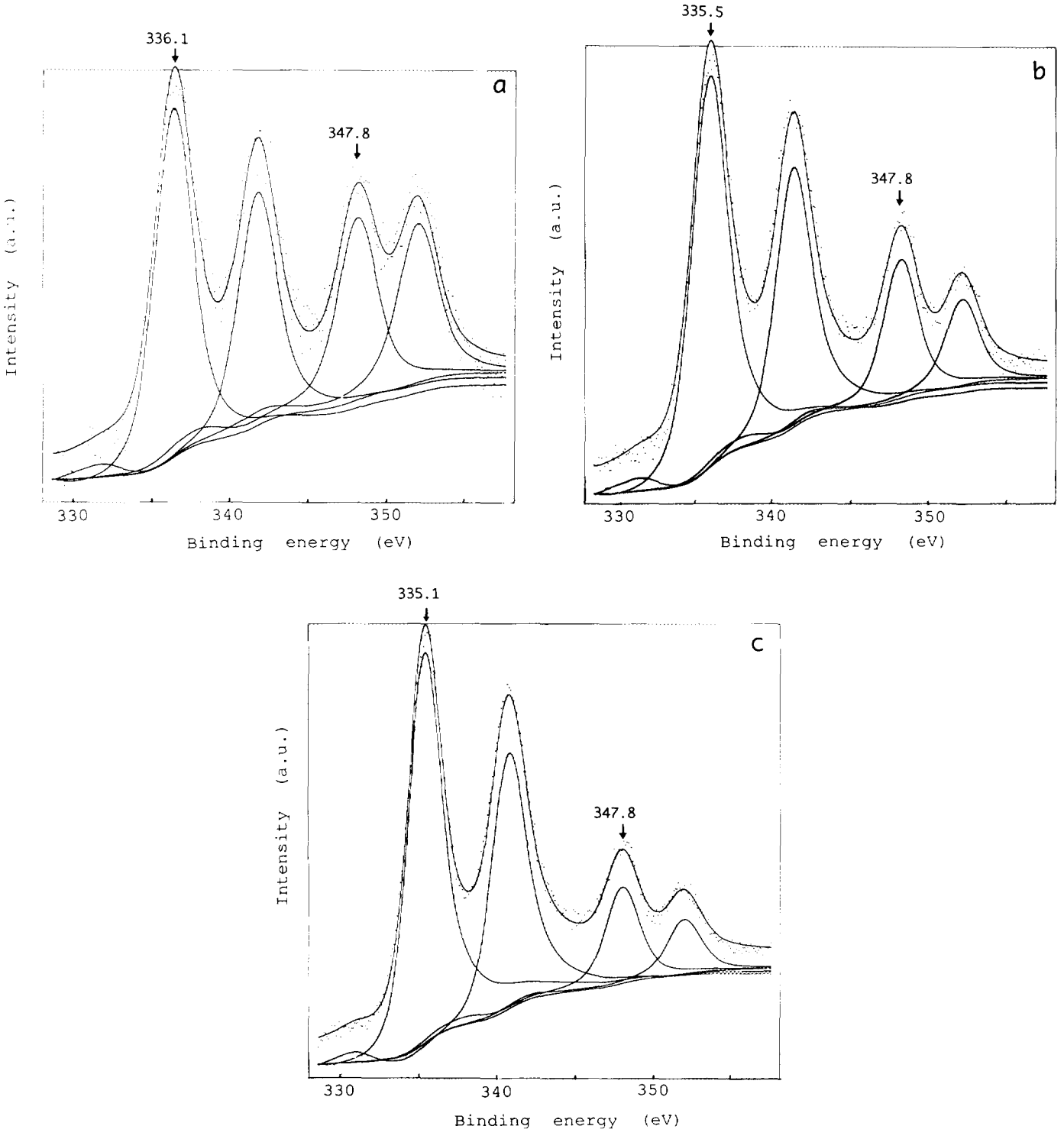

FIG. 2. The curve-fitted palladium 3*d* regions for the Pd/α-Al_2O_3 samples: (a) 0.09 wt%; (b) 0.20 wt%; and (c) 0.30 wt%.

0.2% but the fraction of exposed Pd atoms, after reduction at 573 K, remains constant at 0.50. A further twofold increase in $Pd(C_5H_7O_2)_2$ concentration produced only a 50% increase in metal loading with a marked decrease in dispersion from 0.50 to 0.26. The transmission electron micrograph for the 0.20% sample reduced at 573 K (Fig. 1) indicates a clear bimodal size distribution. Consequently, for this sample the average particle size deter-

TABLE 1

Chemisorption and TEM Characterization for PD/α-Al_2O_3 Catalysts with Different Metal Loadings Reduced at 573 and 773 K

Pd Content (wt%)	Reduction Temperature (K)	Particle size (nm) from: TEM	Particle size (nm) from: $(H/Pd)_{irr}$[a]	Fraction of exposed Pd Atoms from: $(H/Pd)_{irr}$	Fraction of exposed Pd Atoms from: TEM–XPS[c]
0.09	573	2.8[b]	2.1	0.54	0.34
	773	4.5	—	—	0.23
0.20	573	1.4–5.1	2.1	0.52	—
	773	7.7	8.0	0.14	0.16
0.30	573	6.0	4.3	0.26	0.19
	773	7.2	4.9	0.23	0.17

[a] Assuming spherical particles; d(nm) = (1.47*6)/(7.9*H/Pd). From Ref. (34).
[b] Data taken from Ref. (8).
[c] Assuming disk-like particles with diameter d (TEM), height h (XPS) = 3.0 nm, and 1.3×10^{19} surface atoms/m^2.

mined from TEM does not agree with the value calculated from chemisorption measurements, assuming a spherical model. On the contrary, for the other samples the TEM and chemisorption values are closed.

Upon heating at 773 K all samples exhibited a clear particle size increase but this change was more marked for the high dispersion sample. In addition the TEM values for the sintered catalysts were in good agreement with those derived from H_2 chemisorption.

These observations suggest the existence of different Pd phases depending on the metal loading and the H_2 pretreatment temperature.

An EXAFS study by Lesage–Rosenberg *et al.* (16) has shown that the use of $Pd(C_5H_7O_2)_2$ leads to Pd entities anchored to vacant octahedral sites on the γ-Al_2O_3 support. Consequently, extrapolating these results to α-alumina, when the precursor concentration is low the metal will be in a well-dispersed phase with a rather strong metal–support interaction. Increasing the concentration of $Pd(C_5H_7O_2)_2$ produces a parallel, less interactive deposition. The calcination step at 573 K does not alter the fraction of Pd trapped onto the Al_2O_3 support but the less interactive phase is converted to PdO. After reduction two Pd phases would be present, interactive and noninteractive. The bimodal particle size distribution of the 0.20% Pd sample could be explained by the presence of these two phases; when the precursor concentration is still higher, as it was in the 0.30% Pd sample, only noninteractive species could be formed leading to low-dispersed catalysts.

The significant decrease in dispersion observed in the 0.20% sample, treated at 773 K, from H/Pd = 0.52 to H/Pd = 0.14, was consistent with the tendency of Pd particles to sinter in H_2. On the other hand the limited growth of the Pd particles on the 0.30% sample was due to the absence of small particles and the restricted mobility of large crystallites.

On the basis of the above-described results, the concentration of $Pd(C_5H_7O_2)_2$ seems to be a key factor in obtaining different Pd phases supported on α-Al_2O_3. However, it is interesting to recall that other studies have demonstrated the presence of two metal phases on Pd/Al_2O_3 and Pt/Al_2O_3 catalysts, prepared with aqueous precursors (17, 18).

The XPS measurements provided a further insight into the chemical state and morphology of the metal particles. In Table 2, the Pd/Al atomic ratios, deduced from the Pd 3*d* and Al 2*s* line areas (Pd/Al_{XPS}), and the nominal values (Pd/Al_{BULK}) are given for samples treated at 573 and 773 K. It is clear that the Pd/Al_{XPS} values exhibit an approximate linear dependence with the metal concentration whatever the reduction temperature (Fig. 3). According to fundamental XPS studies (19–21), a linear correlation should be expected if the particle size does not vary with the metal loading. However, our TEM data indicate a significant increase in particle size with Pd content. Moreover, when comparing the ratios for each sam-

TABLE 2

Pd/Al Atomic Ratios Determined by XPS for Pd/α-Al_2O_3 Catalysts with Different Metal Loadings Reduced at 573 and 773 K

Pd (wt%)	$Pd/Al_{BULK}(10^4)$	$Pd/Al_{XPS}(10^3)$ 573 K	$Pd/Al_{XPS}(10^3)$ 773 K
0.09	4.31	2.60	2.20
0.20	9.58	6.50	5.90
0.30	14.7	9.00	8.50

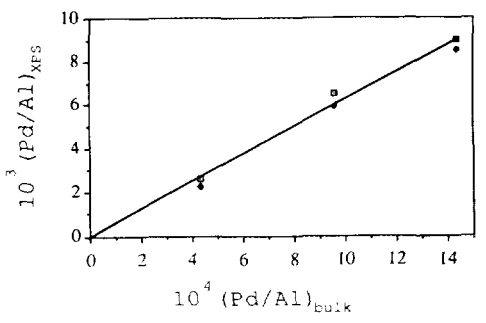

FIG. 3. Pd/Al_{XPS} as a function of Pd/Al_{BULK} intensity ratios for Pd/α-Al_2O_3 samples with different metal loadings reduced at 573 and 773 K: (⊡) 573 K; (◆) 773 K.

ple after the H_2 treatment at 573 and 773 K, one had expected to observe lower values for the catalysts reduced at the highest temperature, since the effective Pd area decreases because of sintering. This phenomenon was not observed in our samples; although TEM and chemisorption data indicated a size variation, the Pd/Al_{XPS} ratio remained almost constant after reduction at high temperature. These discrepancies may be explained if one assumes the presence of flat particles of constant height with the only difference being the particle diameter.

Assuming a disc-like geometry for the Pd particles, it is possible, from XPS signal intensity measurements, to estimate their height. Considering a photoemission process normal to a flat surface, the normalized Pd/Al intensity ratio is related to the metal loading (W), the Pd and Al mean free path (λ), the support surface area (S), and the particle height (h) by the relationship (19)

$$Pd/Al_{XPS} = W(1 - \exp^{-h/\lambda_{Pd}})/[SDh(1 - (W/(SDh)) + (W/(SDh)\exp^{-h/\lambda_{Al}}))],$$

where D is the Pd bulk density. In Fig. 4 the expected variation of Pd/Al with h is shown for the 0.09, 0.20, and 0.30% Pd catalysts. Using the intensity ratios reported in Table 2, the h value for all samples was found to be between 2.5 and 3.6 nm. This value is reasonable.

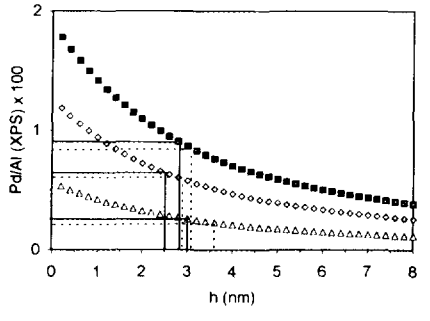

FIG. 4. Theoretical Pd/Al intensity ratios as a function of particle height, assuming disk-like particles, for 0.30 (■), 0.20 (◇), and 0.09 (△) wt% Pd/α-Al_2O_3. The measured Pd/Al_{XPS} values for samples reduced at 573 and 773 K have been indicated: (—) 573 K; (---) 773 K.

If the proposed model is close to reality, it should be adequate to predict the chemisorption results. Assuming a disc-like geometry with height h = 3.0 nm and using the TEM values as particle diameters, the fraction of exposed Pd atoms could be estimated. The results, shown in the last column of Table 1, indicate that the predicted H/Pd ratios are in reasonable agreement with the chemisorption measurements for the samples of low dispersion but reveal that the deviation was larger for the most highly dispersed sample. It is worth noting that the XPS intensity measurements may be affected by contaminants or surface roughness. For example, carbon could decrease the Pd signal compared to Al; therefore a higher Pd/Al_{XPS} intensity ratio would predict a lower h value. We may also question the chemisorption properties of the metal and consequently some discrepancies between chemisorption and the other methods may be expected.

The Pd $3d_{5/2}$ BE are reported in Table 3 as a function of metal loading and reduction temperature. In Fig. 5 the BE values are correlatred with the Pd/Al_{BULK} ratios. Considering the estimated error in BE, 0.1 eV, there were no changes in BE with the reduction temperature, but *a significant upward shift with decreasing metal loading was observed.*

It has been extensively reported that the BE for metal particles on various substrates is a function of particle size; for Pd particles decreasing from 3.0 to 1.0 nm, a BE shift of about 1 eV toward higher BE has been observed (22–28). However, our data in Fig. 5 show high BE values, 336 eV ± 0.1 on samples with 2.8–4.5 nm Pd particles, where bulk metal behavior should have been expected. Furthermore, the H_2 treatment at 773 K produced no change in BE while an increase in particle size occurs. In addition there was a difference of 0.3 eV between the 0.20 and the 0.30% samples reduced at 773

TABLE 3

XPS BE, Auger KE, and Auger Parameter (α_{Auger}) for Pd/α-Al_2O_3 Catalysts with Different Metal Loadings Reduced at 573 and 773 K

	Pd $3d_{5/2}$BE (eV)		Pd MVV Auger KE (eV)		α Auger (eV)	
Pd (wt%)	573 K	773 K	573 K	773 K	573 K	773 K
0.09	336.1	335.9	325.4	325.5	661.5	661.4
0.20	335.5	335.5	325.6	325.8	661.1	661.3
0.30	335.1	335.2	326.3	326.4	661.4	661.6
Estimated error	±0.1		±0.2		±0.3	

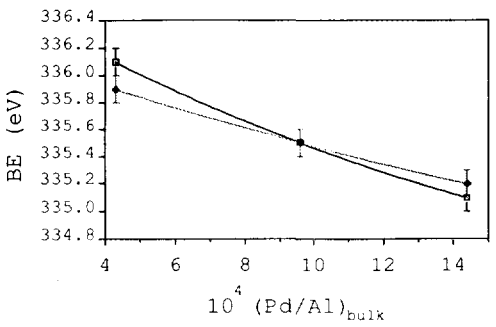

FIG. 5. Pd $3d_{5/2}$ binding energy as a function of metal loading and reduction temperature: (□) 573 K; (◆) 773 K.

K, despite the similar particle size, ~75 Å (see Table 1). Consequently, our results revealed clearly that a particle size effect was not the cause of the observed BE shift.

In the XPS spectra of these low-loaded Pd on alumina catalysts, the Pd Auger lines (Pd MVV) situated in the 1160 eV BE region are broad and superimposed on a steep gradient background. However, since the Pd content was in a similar range for all the samples, a systematic procedure of background subtraction could be applied and the kinetic energies of all the catalytic samples could be compared accurately (Table 3). Then the modified Auger parameter (α_{Auger}) could be estimated (29)

$$\text{XPS BE} + \text{Auger KE} = \alpha_{Auger}.$$

According to Mason (2), the difference in α_{Auger} for Pd in two different environments is twice the difference in the dynamic extraatomic relaxation energy

$$\Delta\alpha = 2\Delta\text{Rex}.$$

As is shown in Table 3, the constance in α_{Auger} values for all the catalysts indicates that the extraatomic relaxation processes are approximately the same. This means that the atoms are in similar chemical environments whatever the catalysts (30). On the other hand, it was determined that differential charging effects generated by the XPS process are ruled out as explained above under Experimental. Therefore it may be concluded that the observed BE shift does not arise from the XPS process (final state) but originates from a peculiar initial state of metal particles in the 0.09% Pd sample, not seen in the 0.3% Pd sample. The presence of interactive and noninteractive particles is again proposed to explain this BE shift.

An interaction between Pd particles and alumina could induce structural changes and/or electronic perturbations. As already suggested (16) we can assume that the particles grow epitaxially with the support and develop (111) monocrystalline particles. In this case, the Pd lines in XPS spectra will appear shifted toward higher BE compared to polycrystalline particles due to the increase in the work function when changing from rugged polycrystalline to dense monocrystalline surfaces. This happens because the BE in our XPS analyses were not referenced to metal Fermi levels but to the support which was independently referenced to the Fermi level of polycrystalline Pd [see Experimental and Ref. (11)]. Some experimental values of work functions compiled in the literature show clearly an increase when the exposed atoms are more and more closely packed, 5.25 eV for Pd(110), 5.65 eV for Pd(100), and 5.95 eV for Pd(111) (31). A lower value, 5.1 eV, has been published for polycrystalline Pd (32). Although the work function variation is largely dependent on the rugosity, the observed 1-eV BE shift is too large to be explained only by this morphological change and electronic perturbations could be also considered.

Joyner *et al.* (33) have shown by theoretical calculations that electronic perturbations at the interface between metal and support extend only a short range, no more than 0.5 nm, into the particle; therefore the majority of Pd atoms in a 3 nm particle would not be influenced by the support as far as electronic properties are concerned. However, it is conceivable that if electrons move from interfacial Pd atoms toward alumina, positive charges would be created and delocalize on the entire surface of the metal particle, giving a positive electrostatic potential to the metal particle, the electric field being nil inside the particle. Then, with XPS analysis, this particle's electrostatic potential would appear as a differential charge effect and lead to an increase in the BE of the metal atoms referenced to the support. Moreover, if the particles are raft-shaped, as proposed above, the interfacial region between metal and support could be considered as a capacitor with a potential ($V = Q/C$) independent of surface area since the capacity, C, and the charge, Q, of such a capacitor would both be proportional to the interfacial surface area. Accordingly similar BE are observed for the 0.09% Pd catalyst reduced at 573 and 773 K while an increase in particle size occurs. Combined structural and electronic changes therefore could explain 1 eV BE shifts between different Pd particles.

At this point of the discussion an adequate interpretation may be given in terms of a metal–support interaction related to the method of preparation. According to the Lesage–Rosenberg model (16) mentioned above, the anchoring of Pd atoms takes place in vacant octahedral aluminium sites forming species close to an aluminate where the metal atoms can be described as Pd^{n+}. After calcination and reduction, Pd particles are formed growing epitaxally with the support. These interactive particles are mainly present in the 0.09% sample. When Pd loading

increases preferential formation of noninteractive particles takes place. Therefore,the BE is shifted to lower binding energy as observed in the 0.20% sample. Furthermore, one can speculate that, in the preparation of the 0.30% sample, the concentration of $Pd(C_5H_7O_2)_2$ is high enough to favor the formation of noninteractive particles against the formation of the "aluminate" to give a BE value of 335.1 eV close to that of pure Pd. Our analysis emphasizes the importance of $Pd(C_5H_7O_2)_2$ concentration to obtain a strong interaction between the metal and the support. In this context it should be mentioned that Pd/Al_2O_3 catalysts, prepared by wet impregnation with $Pd(NO_3)_2$ and reduced at 573 K, give BE values similar to those found on Pd foils (6).

CONCLUSION

A coherent explanation concerning the process of formation of Pd particles on α-Al_2O_3 emerges after a detailed chemisorption, TEM, and XPS study. Using $Pd(C_5H_7O_2)_2$ as a precursor, two different phases may be obtained; in one, Pd is nearly chemically bound at the interface with alumina and in the other, Pd is deposited without bonding. The relative proportion of these two phases will depend on the concentration of $Pd(C_5H_7O_2)_2$. At low concentrations the more interactive phase predominates. Cluster formation during the calcination and/or reduction steps occurs by a growth process that leads to particles of constant height and of varying diameters. An epitaxial growth between the metal and the support leading to formation of (111) monocrystalline particles is proposed. Further studies are needed to describe in detail the interface between particle and metal. Nevertheless, it is worthwhile to insist on the reproducibility of the preparation method leading to the tailoring of interactive and noninteractive particles of palladium deposited on α-alumina. Catalytic reactivity studies currently in progress will analyze the influence of these interactive phenomena.

ACKNOWLEDGMENTS

Many thanks are due to N. Castellani, L. Hilaire, E. Petit, and M. Romeo for stimulating discussions. The authors gratefully acknowledge the CNRS (France) and the CONICET (Argentina) for financial support through the "Progamme International de Coopération Scientifique" (PICS).

REFERENCES

1. Egelhoff, W. F., and Tibbetts, G. G., *Phys. Rev. B* **19,** 5028 (1979).
2. Mason, M. G., *Phys. Rev. B* **27,** 748 (1983).
3. Kohiki, S., and Ikeda, S., *Phys. Rev. B* **34,** 3786 (1986).
4. Cini, M., De Crescenzi, M., Patella, F., Motta, N., Sastry, M., Rochet, F., Pasquali, R., Balzarotti, A., and Verdozzi, C., *Phys. Rev. B* **41,** 5685 (1990).
5. Bastl, Z., *Vacuum* **36,** 447 (1986).
6. Bastl, Z., and Mikusik, P., *Czech. J. Phys. B* **34,** 989 (1984).
7. Boitiaux, J. P., Cosyns, J., and Vasudevan, S., *in* "Proceedings, 3rd Int. Symp. on the Scientific Bases for the Preparation of Heterogeneous Catalysts, Louvain-la-Neuve, 1982," p. 123. Elsevier, Amsterdam, 1983.
8. Aduriz, H. R., Bodnariuk, P., Coq, B., and Figueras, F., *J. Catal.* **119,** 97 (1989).
9. Benson, J. L., Hwang, H. S., and Boudart, M., *J. Catal.*, **30,** 146 (1973).
10. Noack, K., Zbinden, H., and Schlögl, R., *Catal. Lett.* **4,** 145 (1990).
11. Légaré, P., and Fritsch, A., *Surf. Interface Anal.* **15,** 698 (1990).
12. Shirley, D. A., *Phys. Rev. B* **5,** 4907 (1972).
13. Doniach, S., and Sunjic, M., *J. Phys. C* **3,** 285 (1970).
14. Scofield, J. H., *J. Electron. Spectrosc. Relat. Phenom.* **8,** 129 (1976).
15. Légaré, P., and Bilwes, B. R., *Surf. Sci.* **279,** 159 (1992).
16. Lesage-Rosenberg, E., Vlaic, G., Dexpert, H., Lagarde, P., and Freund, E., *Appl. Catal.* **22,** 211 (1986).
17. Yao, H. C., Seig, M., and Plummer, H. K., *J. Catal.*, **59,** 365 (1979).
18. Otto, K., Haack, L. P., and de Vries, J. E., *Appl. Catal. B. Environ.* **1,** 1 (1992).
19. Fung, S. C., *J. Catal.* **58,** 454 (1979).
20. Kerkhof, F. P. J. M., and Moulijn, J. A., *J. Phys. Chem.* **83,** 1612 (1979).
21. Davis, S. M., *J. Catal.* **122,** 240 (1990).
22. Bertolini, J. C., Delichere, P., Khanra, B. C., Massardier, J., Noupa, C., and Tardy, B., *Catal. Lett.* **6,** 215 (1990).
23. Wertheim, G. K., DiCenzo, S. B., and Youngquist, S. E., *Phys. Rev. Lett.* **51,** 2310 (1983).
24. Wertheim, G. K., DiCenzo, S. B., and Buchanan, D. E. N., *Phys. Rev. B* **33,** 5384 (1986).
25. Wertheim, G. K., *Phys. Rev. B* **36,** 9559 (1987).
26. Wertheim, G. K., and DiCenzo, S. B., *Phys. Rev. B* **37,** 844 (1988).
27. Kurt, Ch., and Harsdorf, M., *Surf. Sci.* **245,** 173 (1991).
28. Hub, S., Hilaire, L., and Touroude, R., *Appl. Catal.* **36,** 307 (1988).
29. Wagner, C. D., Gale, L. H., and Raymond, R. H., *Anal. Chem.* **51,** 466 (1979).
30. Wagner, C. D., and Joshi, A., *J. Electron Spectrosc. Rel. Phenom.* **47,** 283 (1988).
31. Wandelt, K., and Gumhalter, B., *Surf. Sci.* **140,** 355 (1984).
32. Jiang, L. Q., Ruckman, M. W., and Strongin, M., *Phys. Rev. B* **39,** 1564 (1989).
33. Joyner, R. W., Pendry, J. B., Saldin, D. K., and Tennison, S. R., *Surf. Sci.* **138,** 84 (1984).
34. Ichikawa, S., Poppa, H., and Boudart, M., *J. Catal.* **91,** 1 (1985).